JOURNAL OF THERMOPHYSICS AND HEAT TRANSFER
Vol. 9, No. 3, July–September 1995

Analysis of Unsteady Forced Convection in Turbulent Duct Flow

C. A. C. Santos,* D. M. Brown,† and S. Kakaç‡
University of Miami, Coral Gables, Florida 33124
and
R. M. Cotta§
Universidade Federal do Rio de Janeiro, Rio de Janeiro 21945-970, Brazil

The results of a theoretical analysis and experimental study of unsteady forced convection with turbulent flow in the thermal entrance region of a circular duct, subjected to a periodically varying inlet temperature, are presented. The related unsteady energy equation for the thermal entrance region is analytically solved under a general boundary condition of the fifth-kind, accounting for the effects of both external convection and wall heat capacitance. Together with empirical models for expressing both eddy viscosity and turbulent velocity profiles, the generalized integral transform technique is used to provide hybrid analytical–numerical solutions for the thermal response of the fluid with a prescribed accuracy. An experimental setup was built and used to validate the mathematical modeling wherein the thermal response of the fluid is obtained in terms of amplitudes and decay indices with respect to the inlet condition for fully developed turbulent flow, due to a sinusoidal variation of the inlet temperature. Satisfactory agreement prevailed between the theoretically and experimentally determined heat transfer characteristics for a succession of axial positions, thereby establishing the theoretical model and numerical technique. To further enhance the model's practical applicability to engineering problems, the analytical technique is extended in obtaining results on the effects of the modified Biot number, fluid-to-wall thermal capacitance ratio, and the Reynolds number, on the thermal response of the fluid within the temperature field, which are presented in tabular forms.

Nomenclature

A = $N \times N$ coefficients matrix defined by Eq. (8b)
$A_{\mathrm{Is},c}(Z)$ = dimensionless temperature amplitude function defined by Eq. (12c)
A_{nk} = coefficient defined by Eq. (7b)
a^* = fluid-to-wall thermal capacitance ratio, $(\rho c_p)_f r_0/(\rho c_p)_w L$
a_{nk} = element of matrix A defined by Eq. (8b)
Bi = modified Biot number, $(h_e r_0)/k$
C_n = coefficient defined by Eq. (8d)
c_p = specific heat, J/(kg·K)
D_h = internal diameter of the test section, $2r_0$, m
$\bar{f}_k$ = coefficient defined by Eq. (7c)
h = outside heat transfer coefficient, W/(m²·K)
h_e = equivalent heat transfer coefficient between wall and ambient fluid at temperature T_∞, $(1/h + L/k_w)^{-1}$, W/(m²·K)
Im = imaginary part of complex value in Eqs. (12c) and (12d)
i = imaginary number, $\sqrt{-1}$
k = thermal conductivity, W/(m·K)
L = tube wall thickness, m
N = number of terms in series
N_k = norm of eigenvalue problem defined by Eq. (6c)
Pr = Prandtl number, (α/ν)
Re = Reynolds number, $(\bar{u}D_h)/\nu$
Re = real part of complex value in Eqs. (12c) and (12d)
r = radial distance, m
r_0 = internal radius of the test section, $(D_h/2)$, m
T = temperature, K
T_∞ = ambient temperature, K
t = time variable, s
$U(R)$ = dimensionless velocity profile
$\bar{u}$ = mean velocity, m/s
$u(r)$ = velocity profile across the duct, m/s
Z = dimensionless axial distance, $(z/D_h)(D_h/r_0)^2/RePr$
z = axial distance, m
α = thermal diffusivity of the fluid, m²/s
β = frequency of inlet oscillations, Hz
ΔT = temperature amplitude, K
$\Delta T(r)$ = inlet temperature amplitude profile
$\Delta\Theta(R)$ = dimensionless inlet temperature amplitude profile
δ_{nk} = for $n = k$, $\delta_{nk} = 1$; for $n \neq k$, $\delta_{nk} = 0$, Eq. (8b)
ε = difference between two values, %
$\Theta_{\mathrm{Is},b}(Z, \tau)$ = dimensionless fluid bulk temperature defined by Eqs. (13a) and (13b)
Θ_n^+ = nth eigenvector for Eq. (8a)
$\tilde{\Theta}(R, Z)$ = quasisteady dimensionless temperature defined by Eq. (4a)
$\Theta(R, Z, \tau)$ = dimensionless temperature defined by Eq. (1a)
λ_n = nth eigenvalue of Eq. (8a)
μ_k = eigenvalue of Eq. (5a)
ν = dynamic viscosity of the fluid, m²/s
ρ = fluid density, kg/m³
τ = dimensionless time, $(\alpha t)/r_0^2$

Received July 19, 1994; revision received Dec. 5, 1994; accepted for publication Dec. 8, 1994.

*Visiting Adjunct Professor, Department of Mechanical Engineering.
†Research Assistant, Department of Mechanical Engineering.
‡Professor and Chairman, Department of Mechanical Engineering.
§Professor, Department of Mechanical Engineering, Cidade Universitaria—CX Postal 68503.

$\phi_{ls,c}(Z)$ = phase lag defined by Eq. (12d)
ψ = eigenfunction of kth eigenvalue defined by Eq. (5a)
Ω = dimensionless inlet frequency, $(\beta r_0^2)/\alpha$

Subscripts
b = bulk temperature
c = centerline of the duct
cs = complete analytical solution
f, w = fluid, wall
ls = lowest-order analytical solution

Introduction

TURBULENT forced convection in ducts is of great interest, as they occur frequently under normal operating conditions for a wide variety of engineering applications, particularly in heating and cooling devices. In heat exchanger applications, the unsteady behavior of temperature distributions can reduce the thermal performance and induce high-level thermal stresses, resulting in catastrophic equipment failure. Therefore, it is important that prior knowledge of temperature and heat flux distributions in unsteady forced convection be known, particularly in turbulent forced convection. This comprehension will permit accurate design of control systems, in addition to providing precise predictions of the thermal, hydraulic, and dynamic analysis of the performance of heat exchange equipment.

A number of research works recently have been reported on transient forced convection inside ducts and channels, especially in laminar flow where the literature can be considered satisfactory, since several papers are available in the open literature on both theoretical analysis and experimental studies. In some of these reported studies, the initial transients are neglected and quasisteady solutions of temperature distributions are used to provide the thermal response of the system under periodic disturbance. Some applications have led to the solutions of complex eigenvalue problems that are not of the conventional Sturm–Liouville type, with the main tasks being finding solutions for the complex eigenvalues and eigenfunctions.

Sparrow and de Farias[1] presented an analysis to the periodic forced convection problem in a parallel-plate channel with sinusoidally varying inlet temperature and slug flow velocity profile, while considering the effects of wall conjugation. Kakaç and Yener[2] obtained an exact solution to the transient energy equation in a parallel-plate channel for a sinusoidal variation of the inlet temperature and slug flow velocity profile. Later, Kakaç[3] obtained a general solution to the transient energy equation subjected to a constant wall temperature or zero wall heat flux boundary condition. The effects of a spatially variable velocity profile were accounted for in the work of Cotta and Özışık,[4] where the generalized integral transform technique was employed to provide analytical solutions. Later, Cotta et al.[5] solved the slug flow problem for circular tubes[1] and parallel-plate channel[2] by developing an approach for complex transcendental equations, and presented accurate results for the related eigenvalues. Ding[6] designed and built a setup and carried out some experimental research. Later, Kakaç et al.[7] compared the experimental findings[6] with theoretical studies for the variation of temperature amplitudes at the centerline of a rectangular duct, subjected to a sinusoidal variation of the inlet temperature under a general fifth-kind of boundary condition, wherein satisfactory comparisons were reported.

Guedes and Cotta[8] used the generalized integral transform technique to solve analytically the transient problem of conjugated convective–conductive heat transfer in laminar flow within a parallel-plate channel under periodic variations of the inlet temperature. Scofano Neto and Cotta[9] extended the ideas in the generalized integral transform technique to obtain analytical solutions for periodic forced convection problems with laminar–laminar and laminar–turbulent flows in concurrent and countercurrent double-pipe heat exchangers. Brown et al.[10–12] carried out a series of experimental and numerical studies on transient laminar and turbulent forced flow inside the thermal entrance region of circular tubes, subjected to periodic variations of inlet temperature under the first-kind of boundary condition. Based on the cases studied, Brown et al.[10–12] proposed an experimentally derived semi-empirical model for correlating the variation of inlet temperature amplitude under steady sustained periodic conditions, for a specified range of Reynolds numbers and frequency of inlet oscillations. Santos and Cotta[13] made use of the generalized integral transform technique to provide an analytical approach to the solution of laminar forced convection inside externally finned circular tubes, subjected to periodic variations of the inlet temperature under a general third-kind of boundary condition and Biot number varying axially. In contrast to laminar flow and its relevance, the literature on turbulent studies remained limited. Quite recently, however, Guedes et al.[14] contributed to the understanding of conjugated periodic turbulent forced convection, through extension of the ideas in the generalized integral transform technique for the parallel-plate configuration.

In the present study, unsteady forced convection with turbulent flow inside the thermal entrance region of a circular duct for a periodic variation of the inlet temperature, subjected to a general fifth-kind of boundary condition is theoretically and experimentally studied. In establishing the theoretical approach, together with the generalized integral transform technique, the fully developed velocity profile is expressed by a three-layer empirical correlation,[15] while the eddy viscosity is defined by a two-layer algebraic model.[16] To assess the accuracy and validity of the present theoretical models, analytical solutions for variation of centerline temperature amplitudes along the duct are compared with the experimental findings at various values of Reynolds numbers and inlet frequencies.

Theoretical Analysis

We consider unsteady forced convection with turbulent flow inside the thermal entrance region of a circular duct subjected to a periodic variation of the inlet temperature. The thermal response of the fluid to the periodic inlet heat input is sought after the initial transients have disappeared. The effects of axial conduction, free convection, and viscous dissipation within the fluid are neglected. Furthermore, assuming that the thermophysical fluid properties remain constant, the unsteady energy equation in the thermal entrance region can be written in dimensionless form as

$$\frac{\partial\Theta(R,Z,\tau)}{\partial\tau} + U(R)\frac{\partial\Theta(R,Z,\tau)}{\partial Z} = \frac{1}{R}\frac{\partial}{\partial R}\left[\varepsilon_h(R)R\frac{\partial\Theta(R,Z,\tau)}{\partial R}\right] \quad \text{for} \quad 0<R<1, \quad Z>0, \quad \tau>0 \tag{1a}$$

with boundary and inlet conditions given, respectively, as

$$\frac{\partial\Theta(R,Z,\tau)}{\partial R} = 0 \quad \text{at} \quad R=0 \quad \text{for} \quad Z>0, \quad \tau>0 \tag{1b}$$

$$\frac{\partial\Theta(R,Z,\tau)}{\partial R} + Bi\Theta(R,Z,\tau) + \frac{1}{a^*}\frac{\partial\Theta(R,Z,\tau)}{\partial\tau} = 0 \quad R=1, \quad Z>0, \quad \tau>0 \tag{1c}$$

$$\Theta(R,Z,\tau) = \Delta\Theta(R)e^{i\Omega\tau} \quad \text{at} \quad Z=0, \quad 0\le R\le 1, \quad \tau>0 \tag{1d}$$

where the various dimensionless groups are defined as

$$\Theta(R, Z, \tau) = \frac{T(r, z, t)}{\Delta T_c} \tag{2a}$$

$$\Delta\Theta(R) = \frac{\Delta T(r)}{\Delta T_c}, \qquad \tau = \frac{\alpha t}{r_0^2}, \qquad R = \frac{r}{r_0}$$

$$\Omega = \frac{\beta r_0^2}{\alpha}, \qquad U(R) = \frac{u(r)}{\bar{u}} = u^+\sqrt{f/8} \tag{2b}$$

$$Bi = \frac{h_c r_0}{k_f}, \qquad Z = (D_h/r_0)^2 \frac{\alpha z}{\bar{u} D_h^2}$$

$$a^* = \frac{(\rho c_p)_f r_0}{(\rho c_p)_w L}, \qquad \varepsilon(R) = 1 + \frac{\varepsilon_h}{\alpha} = 1 + \frac{Pr}{Pr_t}(\varepsilon_m/\nu) \tag{2c}$$

with ε_m being the turbulent eddy viscosity, and u^+ the fully developed turbulent velocity distribution as predicted by the algebraic turbulence model of von Kármán[15] (see Appendix).

Since the present application is concerned only with solutions for large times (i.e., after the initial transients have disappeared), a periodic solution to problem (1) is assumed as

$$\Theta(R, Z, \tau) = \tilde{\Theta}(R, Z)e^{i\Omega\tau} \tag{3}$$

With this approach, an initial condition is not necessary since the solution to the steady-state part of the unsteady temperature response $\tilde{\Theta}(R, Z)$ is sought and system (1) is reduced to

$$U(R)\frac{\partial\tilde{\Theta}(R, Z)}{\partial Z} = \frac{1}{R}\frac{\partial}{\partial R}\left[\varepsilon(R)R\frac{\partial\tilde{\Theta}(R, Z)}{\partial R}\right] - i\Omega\tilde{\Theta}(R, Z)$$

$$0 < R < 1, \qquad Z > 0 \tag{4a}$$

with boundary conditions expressed as

$$\frac{\partial\tilde{\Theta}(R, Z)}{\partial R} = 0 \quad \text{at} \quad R = 0 \quad \text{for} \quad Z > 0 \tag{4b}$$

$$\frac{\partial\tilde{\Theta}(R, Z)}{\partial R} + Bi\tilde{\Theta}(R, Z) + i\Omega\frac{\tilde{\Theta}(R, Z)}{a^*} = 0$$

$$\text{at} \quad R = 1 \quad \text{for} \quad Z > 0 \tag{4c}$$

$$\tilde{\Theta}(R, Z) = \Delta\tilde{\Theta}(R) \quad \text{at} \quad Z = 0 \quad \text{for} \quad 0 \le R \le 1 \tag{4d}$$

The complete numerical solution will depend on the accurate evaluation of eigenvalues and eigenfunctions of the corresponding complex nonclassical Sturm–Liouville problem, due to the complex quantities appearing in both Eqs. (4a) and (4c).

To avoid the complex eigenvalue problem, one can consider the following auxiliary problem:

$$\frac{\mathrm{d}}{\mathrm{d}R}\left[\varepsilon(R)R\frac{\mathrm{d}\psi_k(R)}{\mathrm{d}R}\right] + \mu_k^2 RU(R)\psi_k(R) = 0, \quad 0 < R < 1 \tag{5a}$$

with boundary conditions

$$\frac{\mathrm{d}\psi_k(R)}{\mathrm{d}R} = 0 \quad \text{at} \quad R = 0 \tag{5b}$$

$$\frac{\mathrm{d}\psi_k(R)}{\mathrm{d}R} + Bi\psi_k(R) = 0 \quad \text{at} \quad R = 1 \tag{5c}$$

where $\psi_k(R)$ and μ_k are the eigenfunctions and eigenvalues, respectively. System (5) is solved by the recently advanced sign-count method,[17,18] which provides safe, guaranteed, and automatic computation of as many eigenfunctions and eigenvalues as desired.

With the present approach, the auxiliary eigenvalue problem of system (1) allows definition of the integral transform pair for the function $\tilde{\Theta}(R, Z)$ as

$$\tilde{\Theta}(R, Z) = \sum_{k=1}^{\infty}\frac{\psi_k(R)}{N_k^{1/2}}\overline{\tilde{\Theta}}_k(Z) \tag{6a}$$

$$\overline{\tilde{\Theta}}_k(Z) = \frac{1}{N_k^{1/2}}\int_0^1 RU(R)\psi_k(R)\tilde{\Theta}(R, Z)\,\mathrm{d}R \tag{6b}$$

where a symmetric kernel has been defined, and the normalization integral is expressed as

$$N_k = \int_0^1 RU(R)\psi_k^2(R)\,\mathrm{d}R \tag{6c}$$

The integral transformation of the problem is obtained by operating on Eq. (4a) with

$$\int_0^1 [R\psi_k(R)/N_k^{1/2}]\,\mathrm{d}R$$

to yield a relationship for the temperature field. By manipulating the boundary conditions, Eqs. (4c) and (5c), and using the inversion formula it can be shown that

$$\frac{\mathrm{d}\overline{\tilde{\Theta}}_k(Z)}{\mathrm{d}Z} + \mu_k^2\overline{\tilde{\Theta}}_k(Z) + i\Omega\sum_{n=1}^{\infty}A_{kn}\overline{\tilde{\Theta}}_n(Z) = 0 \tag{7a}$$

where

$$A_{kn} = A_{nk} = \frac{1}{(N_k N_n)^{1/2}}\left[\varepsilon(1)\frac{\psi_k(1)\psi_n(1)}{a^*}\right] + \int_0^1 R\psi_k(R)\psi_n(R)\,\mathrm{d}R \tag{7b}$$

while the inlet condition Eq. (4d) is operated on with

$$\int_0^1 [RU(R)\psi_k(R)/N_k^{1/2}]\,\mathrm{d}R$$

to yield

$$\overline{\tilde{\Theta}}_k(0) = \bar{f}_k = \int_0^1 RU(R)\psi_k(R)\frac{\Delta\Theta(R)}{N_k^{1/2}}\,\mathrm{d}R \tag{7c}$$

System (7) forms an infinite set of coupled, first-order, linear ordinary differential equations, and a closed form solution is unlikely. However, it can be truncated to any sufficiently large order N and solved to the desired accuracy once the related matrix eigenvalue problem has been evaluated for the eigenvalues and eigenfunctions $(\Theta_1^+, \Theta_2^+, \ldots, \Theta_n^+)$ of the $N \times N$ coefficients matrix A, where

$$(A - \lambda_n I)\Theta_n^+ = 0 \tag{8a}$$

with I being a $N \times N$ unit matrix, and

$$A = \{a_{nk}\} \quad \text{and} \quad a_{nk} = \delta_{nk}\mu_n^2 + i\Omega A_{nk} \tag{8b}$$

The complete solution is then constructed from a linear combination of independent solutions expressed, respectively, as

$$\overline{\tilde{\Theta}}_k(Z) = \sum_{n=1}^{N} C_n\Theta_{kn}^+ e^{-\lambda_n Z}, \quad (k = 1, 2, 3, \ldots, N) \tag{8c}$$

in which Θ^{+}_{kn} is the kth component of the nth eigenfunction and the constants C_n are determined from the inlet condition Eq. (7c), as

$$\sum_{n=1}^{N} C_n \Theta^{+}_{kn} = \bar{f}_k, \quad (k = 1, 2, 3, \ldots, N) \tag{8d}$$

System (8) can readily be solved through well-established algorithms for complex problems available in such reliable scientific subroutine packages as the IMSL Library.[19] Once the solution vector Eq. (8c) is obtained at any desired axial position, the inversion formula Eq. (6a) is utilized to produce the complete solution for the temperature field.

As shown in a previous contribution by Santos and Cotta,[13] approximate or lowest-order analytical solutions are readily obtainable from an inspection of the coefficients matrix structure by retaining only the main-diagonal elements [i.e., letting $k = n$ in the infinite summation of Eq. (7a)]. This "so-called" lowest-order analytical solution will be sufficiently accurate for most practical purposes within certain ranges of the parameters governing the relative magnitudes of the main-diagonal elements in the coefficients matrix structure A with respect to elements off the main diagonal. For the present application, this approximation is especially applicable when small values of the dimensionless frequency of inlet oscillations (i.e., for $\Omega \leq 5$) and large values of the fluid-to-wall thermal capacitance ratio a^* are encountered.

When the main-diagonal elements are quite dominant over those off-diagonal elements the approximate, decoupled, or lowest-order system to be solved is written as[13,20]

$$\frac{d\overline{\tilde{\Theta}_{ls,k}}(Z)}{dZ} + (\mu_k^2 + i\Omega A_{kk})\overline{\tilde{\Theta}_{ls,k}}(Z) = 0 \tag{9a}$$

with

$$\overline{\tilde{\Theta}_{ls,k}}(0) = \bar{f}_k \tag{9b}$$

System (9) has an explicit solution of the form

$$\overline{\tilde{\Theta}_{ls,k}}(Z) = \bar{f}_k \exp[-(\mu_k^2 + i\Omega A_{kk})Z] \tag{10}$$

and applying the inversion formula, the thermal response of the fluid within the temperature field can now be stated as

$$\overline{\tilde{\Theta}_{ls}}(R, Z) = \sum_{k=1}^{\infty} \frac{\bar{f}_k}{N_k^{1/2}} \psi_k(R)\exp[-(\mu_k^2 + i\Omega A_{kk})Z] \tag{11}$$

From the definition, the dimensionless temperature along the centerline of the circular duct can now be expressed for the present application as

$$\tilde{\Theta}_{ls,c}(0, Z) = \sum_{k=1}^{\infty} \frac{\bar{f}_k}{N_k^{1/2}} \psi_k(0)\exp[-(\mu_k^2 + i\Omega A_{kk})Z] \tag{12a}$$

which is written in polar form after the time dependence is incorporated as

$$\tilde{\Theta}_{ls,c}(0, Z, \tau) = A_{ls,c}(Z)\exp\{i[\Omega\tau + \phi_{ls,c}(Z)]\} \tag{12b}$$

where the subscripts "ls, c" indicate values derived from the lowest-order analytical technique obtained along the centerline of the circular duct, while $A_{ls,c}(Z)$ and $\phi_{ls,c}(Z)$ are the amplitudes and phase lags, respectively, with respect to the inlet condition and expressed as

$$A_{ls,c}(Z) = \{\mathrm{Re}^2[\tilde{\Theta}_{ls,c}(0, Z)] + \mathrm{Im}^2[\tilde{\Theta}_{ls,c}(0, Z)]\}^{1/2} \tag{12c}$$

$$\phi_{ls,c}(Z) = \tan^{-1}\left\{\frac{\mathrm{Im}[\tilde{\Theta}_{ls,c}(0, Z)]}{\mathrm{Re}[\tilde{\Theta}_{ls,c}(0, Z)]}\right\} \tag{12d}$$

with "Re" and "Im" being the real and imaginary parts, respectively.

For such practical engineering applications, as heat exchanger analysis, another quantity of practical relevance is the evaluation of the local fluid bulk temperature $\Theta_{ls,b}(Z, \tau)$ along the length of the tube, which is computed from its definition as

$$\Theta_{ls,b}(Z, \tau) = \left[\frac{\int_0^1 RU(R)\Theta(R, Z, \tau)\, dR}{\int_0^1 RU(R)\, dR}\right] \tag{13a}$$

or in polar form as

$$\Theta_{ls,b}(Z, \tau) = A_{ls,b}(Z)\exp\{i[\Omega\tau + \phi_{ls,b}(Z)\} \tag{13b}$$

Experimental System

The experiments were performed in an open-circuit suction-type airflow system characterized with a ten-to-one (10:1) convergence ratio bellmouth inlet and an overall effective length of 7.55 m as shown in Fig. 1. An air filter was placed at the entrance of the bellmouth to remove dust particles while simultaneously aiding with flow straightening and reducing the inlet freestream turbulence level. Laboratory air (with controlled relative humidity and dry bulb temperature) was drawn into the setup and passed through the flow development (hydrodynamic inlet) section 4.57 m in length and 7.62 cm in diameter to attain its fully developed velocity profile before entering the electric heater of uniform V-shaped configuration. After leaving the heater, the flowstream entered the thermally developing section (test section) where its thermal characteristics were measured and recorded. The test section of the setup was 3.05 m in length and 7.62 cm in diameter. After exiting the test section, the fluid entered a flow redevelopment section before its passage through the orifice plate and then left the flow circuit through a blower operated in the suction mode.

For the present application, mating ends of the various sections were assembled with the use of rubber sleeves and interface seals. The rubber sleeves acted as shock absorbers and prevented the fan vibration from being propagated to the main sections of the setup. Consistency in alignment of the various sections was maintained by visual inspection of spirit levels together with two pin hole parallelism light sources mounted on the upper and lower surface of the developing and test sections, respectively.

Experimental Procedures

Once the apparatus was assembled and sealed, the fan was activated and the airflow rate adjusted to obtain a predetermined value based on the pressure drop across the orifice plate. The signal generator was switched on, adjusted, and stabilized at a predetermined frequency of the inlet periodic heat input. The power supply was then switched on and the voltage and current levels adjusted to achieve the power required across the heater circuit. During this time, the waveforms of the voltage and current were visually observed on an oscilloscope while hard-copy traces were obtained from a calibrated three-pen strip-chart recorder as a function of paper speed and frequency.

Throughout the investigation, the output from the signal generator was utilized as the controlled input signal to the power supply. This circuitry guaranteed a sinusoidal heat input at the inlet of the thermally developing region (test section). Under steady-sustained periodic inlet conditions, the transient thermal response of the fluid was obtained from the dynamic characteristics of bead-type chromel-constantan thermocouples mounted along the centerline and wall of the test section. The mass flow rate was later evaluated from the pressure drop across the orifice plate manufactured and in-

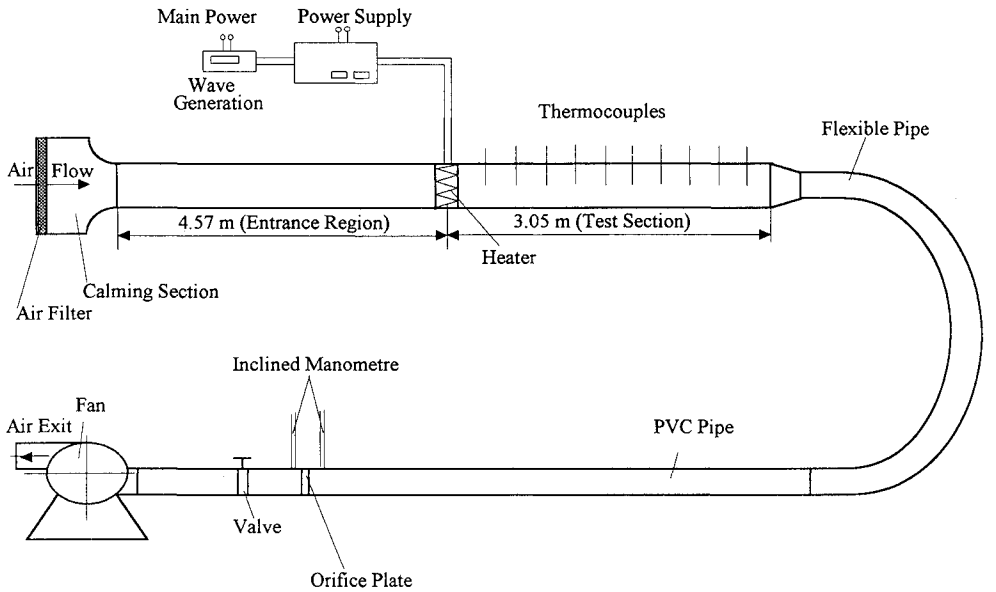

Fig. 1 Schematic diagram of the experimental setup.

stalled in the flow redevelopment section of the apparatus based on ASME standards,[21,22] wherein the change in physical fluid properties due to temperature fluctuations are taken into account. Once the mass flow rate was determined, the Reynolds number in both the redevelopment and test sections were simultaneously evaluated through an iterative procedure, accounting for the effects of compressibility, expansion factor, orifice plate diameter ratio, and the various section geometries. A detailed description of the experimental setup, instrumentation, procedure, and data reduction techniques is given by Ding[6] and Brown.[23]

Experimental Uncertainty

Prior to starting the experimental investigations, all measuring instruments were calibrated and compared with their respective manufacturers' specifications. Furthermore, due to the nature of the investigations, extra care was also exercised when obtaining data of the various experimental parameters. In the present work, temperature measurements are obtained from the dynamic characteristics of standard bead-type chromel–constantan thermocouples by adopting a comparison calibration method. Together with the thermocouples' dynamic characteristics under steady-sustained periodic conditions and the calibration polynomials, the total uncertainty associated with temperature measurement was calculated as ± 0.2°C for the 0–100°C temperature range.

The uncertainty associated with Reynolds number was obtained through the extension of an error propagation model for thin-plate orifice designs,[21,22] wherein variations in physical fluid properties due to temperature changes are considered. Based on the previously mentioned model, the specifications and geometry of the experimental system, the maximum uncertainty associated with Reynolds number was computed as $\pm 2.63\%$.

Results and Discussion

In the theoretical analysis, a formal procedure is presented for obtaining hybrid analytical solutions of unsteady forced convection with turbulent flow inside the thermal entrance region of circular ducts. Furthermore, it is shown that within the periodic state two kinds of solutions are possible, namely, complete and lowest-order, with the complete solution being the more accurate of the two. For the complete analytical solutions, the algebraic eigenvalue problem and the linear system of algebraic equations are solved with the aid of subroutines from the IMSL Library,[19] wherein the functions $\tilde{\Theta}(R, Z)$ are obtained in the form of Eq. (6a). Once the function $\tilde{\Theta}(R, Z)$ has been evaluated, the axial variation in the local fluid bulk temperature and phase lag are simultaneously determined for the temperature field. In the calculation of amplitudes and phase lags of average temperature to four significant figures, the number of terms $N \leq 50$ was sufficient everywhere within the solution domain of the temperature field. However, in most cases, convergence was achieved with 20–30 terms and in regions sufficiently far removed from the very inlet, only few terms were required for convergence.

With the lowest-order analytical technique the eigenvalues (matrix) are not computed, and in such cases the functions of Eq. (11) are referred to as potentials $\tilde{\Theta}_{ls}(R, Z)$. Therefore, it is important to note that although the lowest-order analytic technique will provide explicit approximate solutions, which are useful for fast numerical computations in practical engineering applications, it will only yield accurate results if the main-diagonal elements of the coefficients matrix structure "A" are dominant compared to the off-diagonal elements. In assessing the accuracy and validity of the two theoretical models, the analytical results of the complete solutions are compared with the experimental findings of centerline temperature amplitudes for steady-sustained periodic inlet conditions. For the present application, Bi and a^* were both estimated from available data based on the geometry of the experimental setup, while the inlet temperature amplitude distribution was experimentally determined and introduced in the analytical models. Due to the lower computational cost of the lowest-order technique and its excellent agreement with the complete solution, a comparison is made between the analytic results of both models within the range of the describing variable system parameters, thereby demonstrating the practical relevance and limitations of the lowest-order technique.

In Tables 1 and 2 respectively, comparisons of the variation in amplitudes and phase lags of the local fluid bulk temperature are shown, resulting from the complete and lowest-order analytic techniques. It is shown that the accuracy of the lowest-order solution decreases for large dimensionless distances and large dimensionless frequency of inlet oscillations at a specified Reynolds number. With the complete solution being the basis of comparison, the agreement is shown to be satisfactory over the range of dimensionless inlet frequencies, axial positions, and Reynolds numbers. The associated maximum deviations being 0.71% (Table 1) and 7.76% (Table 2), respectively, for variation in amplitudes and phase lags of the local fluid bulk temperature, occurring at large times and distances far removed from the very inlet.

Table 1 Comparison of the complete and lowest-order solutions for bulk temperature amplitudes

		$A_{cs}(Z)$	$A_{ls}(Z)$	ε, %	$A_{cs}(Z)$	$A_{ls}(Z)$	ε, %	$A_{cs}(Z)$	$A_{ls}(Z)$	ε, %	$A_{cs}(Z)$	$A_{ls}(Z)$	ε, %
6,185	0.558	0.3186	0.3186	0.00	0.2620	0.2620	0.00	0.2363	0.2363	0.00	0.2121	0.2121	0.00
6,202	4.464	0.3186	0.3186	0.00	0.2614	0.2619	0.19	0.2352	0.2363	0.47	0.2105	0.2121	0.76
19,740	0.558	0.3036	0.3036	0.00	0.2541	0.2541	0.00	0.2369	0.2369	0.00	0.2255	0.2255	0.00
19,770	4.464	0.3036	0.3036	0.00	0.2540	0.2541	0.04	0.2367	0.2369	0.08	0.2252	0.2255	0.13

Table 2 Comparison of the complete and lowest-order solutions for phase lag of bulk temperature amplitude

		ϕ_{cs} $\times 10^3$	ϕ_{ls} $\times 10^3$	ε, %	ϕ_{cs} $\times 10^3$	ϕ_{ls} $\times 10^3$	ε, %	ϕ_{cs} $\times 10^3$	ϕ_{ls} $\times 10^3$	ε, %	ϕ_{cs} $\times 10^3$	ϕ_{ls} $\times 10^3$	ε, %
6,185	0.558	0.4493	0.4144	7.76	4.940	4.588	7.13	9.469	9.049	4.44	15.11	14.68	2.85
6,202	4.464	3.585	3.307	7.75	39.39	36.61	7.06	75.49	72.21	4.34	120.4	117.1	2.74
19,740	0.558	0.4184	0.1429	3.71	1.655	1.562	5.62	3.169	3.043	3.98	5.049	4.915	2.65
19,770	4.464	1.186	1.142	3.71	13.22	12.48	5.59	25.32	24.31	3.99	40.43	39.27	1.16

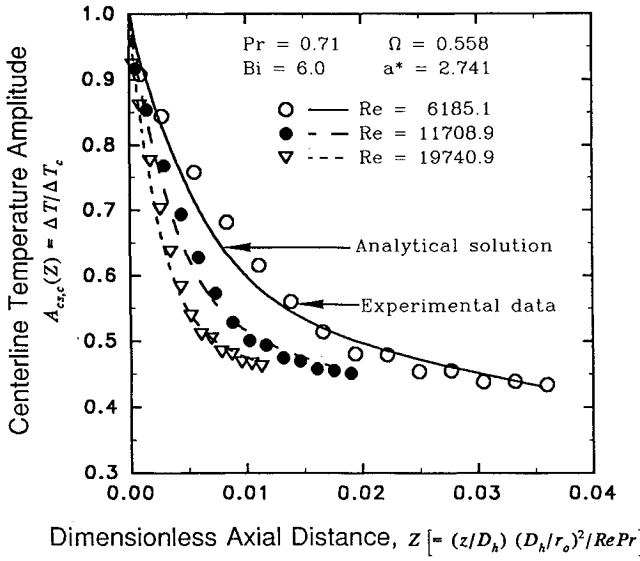

Fig. 2 Theoretical and experimental centerline temperature amplitude as a function of dimensionless streamwise coordinate. Ω = 0.558.

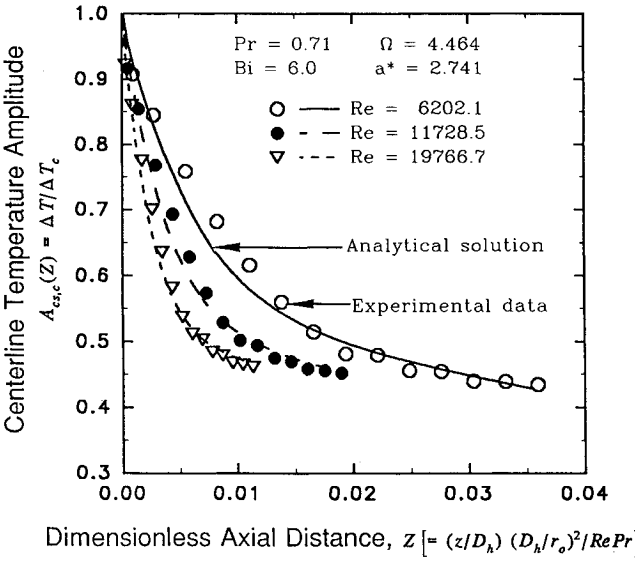

Fig. 3 Theoretical and experimental centerline temperature amplitude as a function of dimensionless streamwise coordinate. Ω = 4.464.

Although the previously cited comparisons are satisfactory, the limitations to the accuracy of the lowest-order analytic technique in the calculation of heat transfer characteristics, resulting from the restriction imposed on the coefficients matrix structure, should be recognized. The solution of the original complex problem was transformed to the solution of an infinite set of coupled, first-order, linear ordinary differential equations, wherein the lowest-order solution is defined as that which is developed from the results of the decoupled form. If the coefficients matrix of the system of equations were a diagonal matrix, then the system would be decoupled. Therefore, an accurate prediction of the fluid's thermal response within the temperature field by the lowest-order technique can only be achieved when the main-diagonal elements are dominant compared to the off-diagonal elements. In addition, the diagonally dominant characteristic of the coefficients matrix structure must hold for the time periods that solutions are sought, and at all values of such describing variable fluid parameters, as Reynolds number, frequency of inlet oscillation, and axial position.

Figures 2 and 3 show the variation in amplitudes of the centerline fluid temperature as a function of the dimensionless streamwise coordinate for two different inlet frequencies and at three different Reynolds numbers. The results of the complete analytic solutions (shown as solid and broken lines), are superimposed on the experimental findings (expressed with symbols). As illustrated in the figures, the amplitude of the centerline temperature takes on its maximum value at the inlet of the duct and then decreases monotonically with increasing downstream distance. The rate of decrease is observed to be sharp in the immediate neighborhood of the inlet, but becomes more gradual as the curves tend to level off and the amplitudes of the thermal oscillations approach their minimum values. The extent of dropoff is shown to increase as the Reynolds number increases, wherein an exponential trend is observed in the decaying amplitudes of the thermal oscillations along the centerline of the duct. This observation is typical of both theoretical and experimental studies. In general, amplitudes of the centerline fluid temperature are observed to be larger than those of local fluid bulk temperature for similar axial positions and flow conditions as illustrated in Figs. 2 and 3, and Table 1, respectively.

For the range of Reynolds numbers and frequency of inlet oscillations considered, an overall inspection of Figs. 2 and 3 show that excellent agreement prevails between the experimentally and analytically determined centerline temperature amplitudes for a succession of axial positions along the duct. For the majority of points the agreement is within 1.5%, with the maximum deviation being 2.3% occurring at the lowest Reynolds number and frequency of inlet temperature oscillation. The excellent agreement provides confidence in the capabilities of the analytical models and numerical technique in predicting the thermal response of the fluid within the temperature field with prescribed accuracy under periodic inlet conditions.

An inspection of Figs. 4 and 5 reveals that a linear functional relationship characterizes the variation in phase lag of centerline temperature amplitudes with distance along the duct.

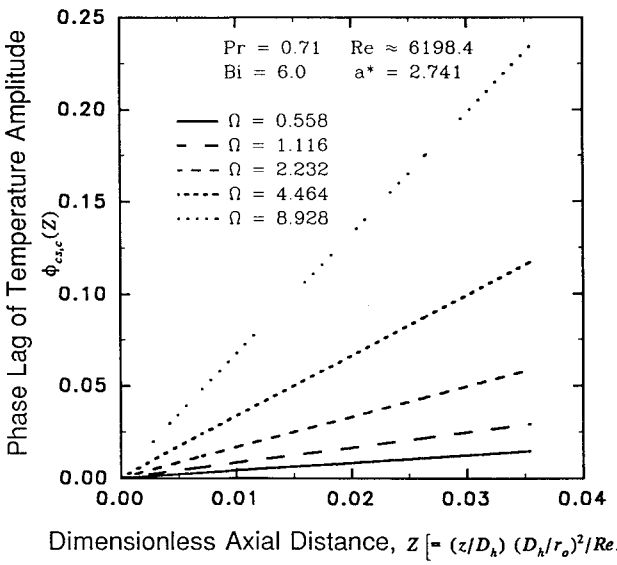

Fig. 4 Variation in phase lag of centerline temperature amplitude as a function of dimensionless streamwise coordinate. $Re \approx 6.1984 \times 10^3$.

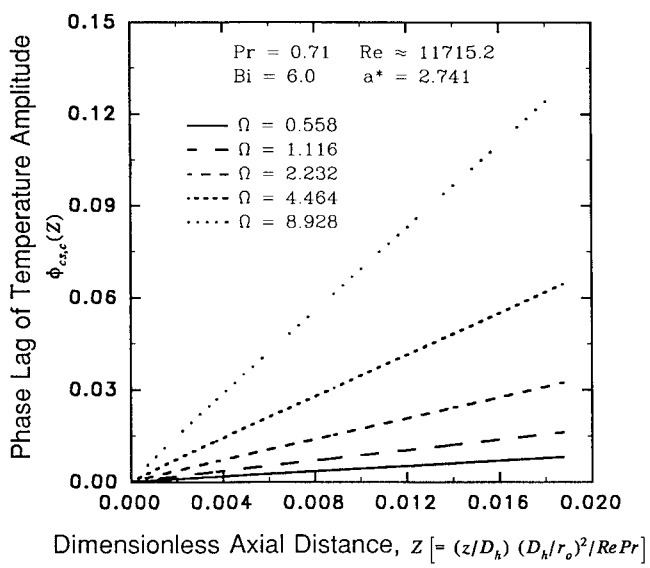

Fig. 5 Variation in phase lag of centerline temperature amplitude as a function of dimensionless streamwise coordinate. $Re \approx 1.17152 \times 10^4$.

At a specified Reynolds number, the phase lag increases with increased inlet frequencies and downstream distance. Furthermore, variations in phase lag associated with centerline temperature amplitudes are shown in Figs. 4 and 5 to decrease with increased Reynolds number at a given value of the inlet frequency and position along the duct. This behavior of the fluid's transient thermal response is indicative of increased phase lags with increased dimensionless frequency of inlet oscillation, as shown in Table 2. For the cases considered and at corresponding downstream distances, although a linear function characterized the distributions of Figs. 4 and 5, it is observed that the phase lags associated with amplitudes of bulk temperature are less than those associated with amplitudes of centerline temperature.

Consequently, if at a specified Reynolds number and increasing dimensionless frequency the heat capacity of the fluid can be regarded as a controlling factor that governs the thermal response within the temperature field, then, for such cases the thermal storage in the fluid will delay the response sensed at each axial downstream location, with respect to the inlet disturbance carried by the thermal oscillations. Subsequently, for a given value of the dimensionless inlet frequency if an increase of the Reynolds number represents an increased fluid velocity, the fluid with a higher Reynolds number will transfer the inlet disturbances carried by the thermal wave more rapidly than one with a lower Reynolds number. In such cases, the phase lag will decrease as the Reynolds number is increased at a specified frequency of inlet oscillation. This unsteady phenomena is illustrated in Table 2 and the plots of Figs. 4 and 5.

Conclusions

A methodology, based on the ideas associated with the generalized integral transform technique, is presented for developing analytic solutions to unsteady forced flow inside circular ducts. To illustrate the application, consideration is given to unsteady forced convection with turbulent flow inside the thermal entrance region of a smooth circular duct, subjected to periodic variations of the inlet temperature under a general fifth-kind of boundary condition.

In assessing the accuracy and validity of the theoretical models, the complete and lowest-order analytical solutions for the periodic state are shown to be in satisfactory agreement with experimental findings. The lowest-order analytical technique, although subjected to restrictions of the coefficients matrix structure, has demonstrated its practical potential and applicability in obtaining fast numerical computations of heat transfer characteristics in the solution of engineering problems.

Appendix

We may empirically express the fully developed turbulent velocity profile by a three-layer model according to von Kármán,[15] as

$$u^+ = y^+ \quad \text{for the viscous sublayer,} \quad 0 < y^+ < 5 \tag{A1}$$

$$u^+ = 5.0\,\ln[(1 - R)R^+] - 3.05$$

$$\text{for the buffet layer,} \quad 5 \le y^+ \le 30 \tag{A2}$$

$$u^+ = 2.5\,\ln\left[\frac{1.5(1 - R^2)R^+}{1 + 2R^2}\right]$$

$$\text{for the turbulent core,} \quad y^+ > 30 \tag{A3}$$

where $y^+ = \frac{1}{2}(1 - R)Re\sqrt{f/8}$ and $R = 1 - (y^+/R^+)$.

For turbulent convective heat transfer, it is essential to know the eddy viscosity ε_m and the thermal eddy diffusivity ε_h. In this analysis, a two-layer algebraic model is applied, and the eddy viscosity is expressed as

$$\frac{\varepsilon_m}{\nu} = \frac{K}{E}\left[(e^{-Ku^+} - 1) - Ku^+ - \frac{(Ku^+)^2}{2!} - \frac{(Ku^+)^3}{3!}\right]$$

$$\text{for} \quad y^+ < 40 \tag{A4}$$

while

$$\varepsilon_m/\nu = (KR^+/6)(1 - R^2)(1 + 2R^2) \quad \text{for} \quad y^+ \ge 40 \tag{A5}$$

where the model constants are respectively given as $K = 0.407$ and $E = 10.0$ by Spalding[16] and the turbulent Prandtl number Pr_t is expressed as $Pr_t = \varepsilon_m/\varepsilon_h$.

According to the experiments of Larson and Yerazunis,[24] for fluids with $Pr = 0.70$, the turbulent Prandtl number can generally be assumed constant and taken as $Pr_t = 0.86$.

Acknowledgments

C. A. C. Santos acknowledges the support from CNPQ and UFPB of Brazil. The partial financial support of the U.S. National Science Foundation and NATO Scientific Affairs Division is also acknowledged.

References

[1]Sparrow, E. M., and De Farias, F. N., "Unsteady Heat Transfer in Ducts with Time Varying Inlet Temperature and Participating Walls," *International Journal of Heat and Mass Transfer*, Vol. 11, No. 5, 1968, pp. 837–853.

[2]Kakaç, S., and Yener, Y., "Exact Solution of the Transient Forced Convection Energy Equation for Timewise Variation of Inlet Temperature," *International Journal of Heat and Mass Transfer*, Vol. 16, No. 2, 1973, pp. 2205–2214.

[3]Kakaç, S., "A General Solution to the Equation of Transient Forced Convection with Fully Developed Flow," *International Journal of Heat and Mass Transfer*, Vol. 18, No. 12, 1975, pp. 1449–1453.

[4]Cotta, R. M., and Özışık, M. N., "Laminar Forced Convection Inside Ducts with Periodic Variation of Inlet Temperature," *International Journal of Heat and Mass Transfer*, Vol. 29, No. 10, 1986, pp. 1495–1501.

[5]Cotta, R. M., Mikhailov, M. D., and Özışık, M. N., "Transient Conjugated Forced Convection in Ducts with Periodically Varying Inlet Temperature," *International Journal of Heat and Mass Transfer*, Vol. 30, No. 10, 1987, pp. 2073–2082.

[6]Ding, Y., "Experimental Investigation of Transient Forced Convection in Ducts for a Timewise Varying Inlet Temperature," M.S. Thesis, Univ. of Miami, Miami, FL, 1987.

[7]Kakaç, S., Li, W., and Cotta, R. M., "Unsteady Laminar Forced Convection in Ducts with Periodic Variation of Inlet Temperature," *Journal of Heat Transfer*, Vol. 112, No. 4, 1990, pp. 913–920.

[8]Guedes, R. O. C., and Cotta, R. M., "Periodic Laminar Forced Convection Within Ducts Including Wall Heat Conduction Effects," *International Journal of Engineering Science*, Vol. 29, No. 5, 1991, pp. 535–547.

[9]Scofano, N. F., and Cotta, R. M., "Dynamic Analysis of Double Pipe Heat Exchangers Subjected to Periodic Inlet Temperature Disturbances," *Warme-und-soffubertragung*, Vol. 28, No. 8, 1993, pp. 497–503.

[10]Brown, D. M., Li, W., and Kakaç, S., "Unsteady Laminar Forced Convection in Circular Ducts with Periodic Variation of Inlet Temperature," *Proceedings of the 29th National Heat Transfer Conference*, HTD-Vol. 237, 1993, pp. 103–110.

[11]Brown, D. M., Li, W., and Kakaç, S., "Numerical and Experimental Analysis of Unsteady Heat Transfer with Periodic Variation of Inlet Temperature in Circular Ducts," *International Communications in Heat and Mass Transfer*, Vol. 20, No. 6, 1993, pp. 883–899.

[12]Brown, D. M., Li, W., and Kakaç, S., "Experimental Study of Fully Developed Laminar and Turbulent Transient Thermal Entrance Heat Transfer in Circular Ducts," *Proceedings of the 1st ISHMT–ASME Heat and Mass Transfer Conference*, HMT-94-032, 1994, pp. 257–263.

[13]Santos, C. A. C., and Cotta, R. M., "Dynamic Analysis of Heat Exchangers with Externally Finned Tubes," *Proceedings of the International Symposium on New Development in Heat Exchangers*, Inst. Superior Técnico, Lisbon/Portugal, 1993.

[14]Guedes, R. O. C., Özışık, M. N., and Cotta, R. M., "Conjugated Periodic Turbulent Forced Convection in a Parallel Plate Channel," *Journal of Heat Transfer*, Vol. 116, No. 1, 1994, pp. 40–46.

[15]Von Kármán, T., "Mechanische Ähnlichkeit und Turbulenz," *Nachr. Ges. der Wiss. Göttingen, Mathematical Physics Klasse*, Vol. 58, No. 5, 1930, pp. 58–76; also NACA TM 611, 1931.

[16]Spalding, D. B., "A Single Formula for the 'Law of the Wall,'" *Journal of Applied Mechanics*, Vol. 28, Sept. 1961, pp. 455–457.

[17]Mikhailov, M. D., and Özışık, M. N., *Unified Analysis and Solutions of Heat and Mass Diffusion*, Wiley, New York, 1984, pp. 115–122.

[18]Mikhailov, M. D., and Vulchanov, "Computational Procedure for Sturm-Liouville Problems," *Journal of Computational Physics*, Vol. 50, No. 3, 1983, pp. 323–336.

[19]IMSL Library, 7th GNB Building, 7500 Ballaire Blvd., Houston, TX, 1979.

[20]Cotta, R. M., "Integral Transforms in Computational Heat and Fluid Flow," CRC Press, Boca Raton, FL, 1993.

[21]"Measurement of Fluid Flow in Pipe Using Orifice, Nozzle and Venturi," American Society of Mechanical Engineers Standards MCF-3M, 1984.

[22]"Fluid Meters; Their Theory and Applications," American Society of Mechanical Engineers Standards, 1971.

[23]Brown, D. M., "Experimental Investigation of Transient Forced Convection in a Circular Duct for Timewise Variation of Inlet Temperature," M.S. Thesis, Univ. of Miami, Miami, FL, 1992, pp. 46–107.

[24]Larson, R. I., and Yerazunis, S., "Mass Transfer in Turbulent Flow," *International Journal of Heat and Mass Transfer*, Vol. 16, No. 1, 1973, pp. 121–128.